J. Physiol. (1981), **316**, *pp.* 503–525
With 15 text-figures
Printed in Great Britain

3-*O*-METHYLGLUCOSE TRANSPORT IN INTERNALLY DIALYSED GIANT AXONS OF *LOLIGO*

BY P. F. BAKER AND A. CARRUTHERS
From the Department of Physiology, King's College, Strand, London WC2R 2LS

(*Received 14 July 1980*)

SUMMARY

1. The transport of the non-metabolized sugar, 3-*O*-methylglucose, has been studied in the squid axon under conditions where the intracellular environment of the axon is controlled by internal dialysis.

2. Sugar transport is passive, shows saturation kinetics and is asymmetric. At 15 °C, the Michaelis and velocity constants for exit are approximately four times those for uptake. The asymmetry of transport is increased by raising the temperature.

3. Sugar uptake is not affected by intracellular sugar levels as high as 100 mM. Sugar exit is, however, reduced by external sugars although the apparent K_m for exit is unaffected.

4. The kinetics of sugar exit under exchange conditions are determined by the kinetics of sugar uptake. These results can be accounted for by the asymmetric mobile-carrier and simultaneous-carrier models for transport.

5. Both sugar uptake and exit are reduced in the absence of ATP_i. Kinetic analysis of transport under these conditions shows that the capacity of the system to transport sugar is unchanged but that the affinity of the system for sugar is reduced. Internal cyclic AMP, AMP, ADP or GTP (2 mM) do not mimic this action of ATP. The hydrolysable analogue of ATP, α, β-methylene-5-ATP (2 mM), (but not the non-hydrolysable analogue β, γ-methylene-5-ATP, 2 mM) has an ATP-like action on sugar transport.

6. Transport is unaffected by internal Ca^{2+} concentrations in the range $4 \times 10^{-8} - 9 \times 10^{-7}$ M.

INTRODUCTION

The squid axon has many attractive features for studying the detailed properties of sugar transport in nervous tissue. Not only are there close similarities between the sugar transport system of squid axons and mammalian preparations (Baker & Carruthers, 1981), but the large size of the squid axon makes possible a level of experimental analysis that is extremely difficult in much smaller mammalian cells.

One such approach is the measurement of fluxes under conditions where the ionic environment on both sides of the plasma membrane is under experimental control (Baker, Hodgkin & Shaw, 1962; Brinley & Mullins, 1967). In this paper we examine the kinetics of transport of the non-metabolized sugar 3-*O*-methylglucose in axons where the intracellular axoplasmic compartment is controlled by dialysis. The

transport system for 3-*O*-methylglucose is saturable, passive, asymmetric and sensitive to ATP.

METHODS

Materials. The hindmost stellar giant axons from *Loligo forbesi* were used throughout. Axons were normally taken from large living squid but occasionally were dissected from mantles stored in refrigerated sea water for 2–5 h. All fibres were cleaned carefully to remove adhering connective tissue and small nerve fibres. Mean axon diameter was 794 ± 22 μm ($n = 36$). All experiments were carried out at 15 °C.

Solutions

External solutions. The composition of the sea water was (mM): NaCl, 400; KCl, 10; $MgCl_2$, 100; $CaCl_2$, 10; $NaHCO_3$, 2·5; pH 7·8. 3-*O*-methylglucose was added to the sea water in appropriate amounts and made radioactive by addition of ^{14}C-labelled 3-*O*-methylglucose. The increase in 3-*O*-methylglucose concentration on adding isotope was less than 100 μm.

Internal solutions. The composition of the internal dialysis solution was as follows (mM): K glutamate, 300; Na aspartate, 80; $MgCl_2$ (in excess of Mg-ATP), 5; $CaCl_2$, 1·5; EGTA, 5; taurine, 275; Hepes, 5; Pipes, 10; NaCN, 2; carbonylcyanide-*p*-trifluoromethoxyphenylhydrazone (FCCP), 2 μg/ml; Mg-ATP, 4; pH, 7·2. The Na concentration used in all experiments (80 mM), although higher than that occurring in axoplasm extruded from axons taken from living squid, was considered to be closer to the Na content of axoplasm in most of our experiments on intact axons obtained from refrigerated mantles. A ratio of 3:10 Ca:EGTA was used to maintain free Ca levels close to physiological values (Baker, Hodgkin & Ridgway, 1971). Cyanide and FCCP were added to block ATP synthesis and Ca accumulation by mitochondria. This solution was stored at −22 °C. ATP (4 mM) was added to the solution immediately before each experiment as Mg-ATP and the pH adjusted to 7·2. 3-*O*-methylglucose and 3-*O*-methyl-α-D-[U-^{14}C]glucose were added to the solution in appropriate amounts. Unless stated otherwise, the concentration of ATP in all experiments was 4 mM.

Internal dialysis

The principle of the method and the use of porous cellulose acetate tubing in internal dialysis have been described elsewhere (Brinley & Mullins, 1967).

Preparation of the porous capillary. Cellulose acetate tubing (o.d. 130 μm, wall thickness 20 μm) was rendered porous over a defined length (2 cm) by soaking in 50 mM-NaOH for 24 h. The porosity of the capillaries was checked by the method of Brinley & Mullins (1967) and the results showed that for ionic and molecular species of less than 600 daltons the coefficient for diffusion through the capillary was some 15% of that in aqueous solution.

Insertion of the porous capillary. The finely cleaned axon was cannulated at each end and mounted, horizontally, in a Perspex chamber. The dialysis capillary, which had been strengthened by insertion of a length of straightened tungsten wire (diameter = 70 μm), was threaded carefully through the fibre. Care was taken to keep the tip of the capillary in the centre of the fibre; this was facilitated by placing a front surface mirror at 45° to the fibre. Once in position a flow of dialysis solution was established through the tubing and the tungsten wire withdrawn. Flow through the capillary was about 2 μl . min^{-1}. Normally an axial electrode was inserted into the fibre before the dialysis capillary to ensure that no great damage was done to the membrane on insertion of the tubing. With care, insertion of the capillary caused only a slight depolarization of the membrane (2–3 mV). Mean membrane potential was $-53{\cdot}7 \pm 2{\cdot}8$ mV ($n = 24$) (not corrected for tip potentials).

Efflux measurements. Isotope was added to the internal solution and the fibres superfused with sea water at a rate of 0·66 ml . min^{-1}. Isotope supplied in this way also enters those regions of the nerve which are less completely dialysed at each end of the porous section of the dialysis capillary. To avoid collecting isotope from these sections of the nerve a guard system was operated (see Fig. 1*A*). By slowly withdrawing sea water superfusing these sections of the fibre it can be shown that isotope which is collected from the centre of the chamber comes only from the well dialysed portion of the axon.

Samples were collected every 5 min and counted. All counts were corrected for quenching.

Influx measurements. Influx measurements were made by adding radioactive sugar to the sea water and collecting the isotope emerging at the tip of the porous capillary. Reliable measurements of influx are less easily made than efflux measurements because of the accumulation of isotope in

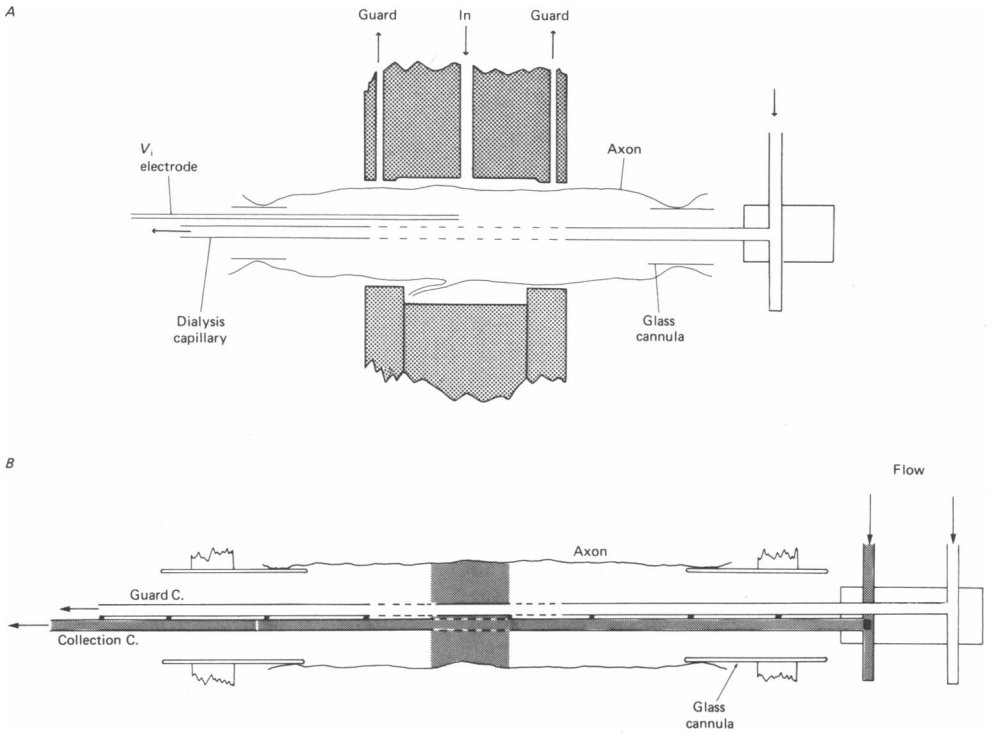

Fig. 1. Experimental arrangement for internal dialysis. *A*, *efflux*: a single dialysis capillary is inserted into the fibre via the right hand cannula and E_M recording electrode via the left cannula. The porous section of the dialysis tubing is shown by the dashed lines. The fibre is superfused with sea water and a guard system operated to collect isotope entering the central compartment from the less well dialysed end regions of the fibre. Fluid was withdrawn from the central compartment to maintain the fluid level constant. *B*, *influx*: schematic view of the double-barrelled dialysis capillary in position inside an axon (not to scale). Both capillaries are mounted in a Perspex block and separate flow to each capillary is delivered by motor-driven syringes. The porous section of each capillary is shown by the dashed lines. When phenol red is added to the solution flowing through the collection capillary a sharp cut off in the colouration of axoplasm is seen on either side of the porous region of the collection capillary. When the guard capillary flow is halted, the colouration spreads beyond the region of axoplasm dialysed by the collection capillary.

the less well dialysed regions of the fibre. To avoid this a double-barrelled dialysis capillary was constructed (Brinley, Spangler & Mullins, 1975; see Fig. 1 *B*). The collection capillary was as normal but a guard capillary, rendered porous on either side of the porous section of the collection capillary, was cemented alongside it. Dialysis fluid was flowed through both capillaries at the same rate. The guard capillary effectively dialyses out isotope that enters the axon at both ends of the porous section of the collection capillary. When phenol red was included in the solution flowed through the collection capillary, a sharp cut-off in the colouration of axoplasm was always seen at each end of the porous section of the collection capillary (see Fig. 1 *B*). The time course for the loss of isotope from axoplasm with the guard 'on' was similar to the time course of reaching a steady state of influx on addition of isotope to the external solution, suggesting that accumulation of isotope in end regions is avoided by use of the guard.

Success in controlling the intracellular environment. Fig. 2 shows a recording of membrane potential in a dialysed fibre with the tip of the electrode positioned as close to the membrane as possible without causing damage. When the fibre was superfused with 10 mM-KCl sea water and 200 mM of the 300 mM internal K glutamate replaced with 200 mM-Na glutamate the membrane

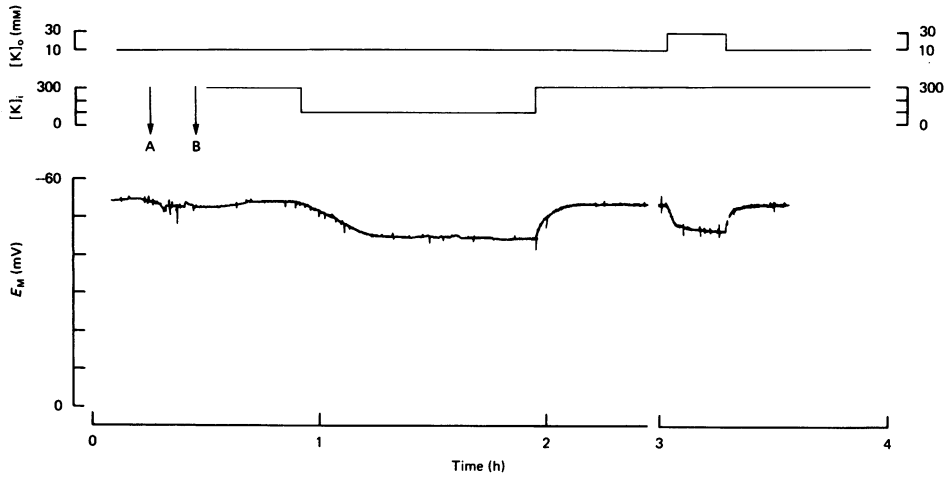

Fig. 2. Control of solute composition of axoplasm: the effect on membrane potential of replacing two-thirds of the internal K glutamate with Na glutamate. Ordinate: membrane potential corrected for junction potentials. Abscissa: time in h. A marks the time of dialysis capillary insertion and B the onset of dialysis with artificial medium. Internal and external K concentrations are shown above the record. Temperature, 15 °C; axon diameter, 680 μm. Fibre was kept at 4 °C for 12 h before use.

depolarization was equivalent to the depolarization seen when external K was increased to 30 mM with 300 mM-K glutamate internally. The depolarization was fully developed within 20 min of reducing internal K and full recovery was seen within 18 min of returning to 300 mM internal K.

On addition of ^{14}C-labelled 3-*O*-methylglucose to either the external or internal solutions, sugar uptake or exit normally reaches a steady level after about 40 min with a half-time of 3–6 min. This is much slower than would be expected from the measurements of the radial self-diffusion of 3-*O*-methylglucose in axoplasm (Baker & Carruthers, 1981). This discrepancy arises because the diffusion of sugar through the porous dialysis capillary is only some 15 % of that in aqueous solution.

*Analyses of data in terms of kinetic models for the transfer of 3-*O*-methylglucose across the axolemma*

During the course of this work it became clear that the transport of 3-*O*-methylglucose in the squid giant axon could be accounted for both by the asymmetric form of the mobile carrier (Widdas, 1952, 1980; Geck, 1971) and by an asymmetric two-component simultaneous carrier (Baker & Widdas, 1973). These two types of model are described in Fig. 3. The equation describing the unidirectional efflux ($V_{1\to2}$) of sugar on a mobile-carrier from a cell is given by Lieb & Stein (1974) as

$$V_{1\to2} = \frac{K_{21}P + PQ}{K_{12}K_{21}R_{oo} + K_{21}R_{12}P + K_{12}R_{21}Q + R_{ee}PQ} \tag{1}$$

where P and Q refer to the intracellular and extracellular sugar concentrations respectively, and in the absence of unstirred layers

$$R_{12} = \frac{1}{V^{zt}_{1\to2}}; \quad R_{21} = \frac{1}{V^{zt}_{2\to1}}; \quad R_{ee} = \frac{1}{V^{ee}}$$

$$K^{zt}_{1\to2} = \frac{K_{12}R_{oo}}{R_{12}}; \quad K^{zt}_{2\to1} = \frac{K_{21}R_{oo}}{R_{21}}; \quad K^{ic}_{1\to2} = \frac{K_{21}R_{12}}{R_{ee}}$$

$$K^{ic}_{2\to1} = \frac{K_{12}R_{21}}{R_{ee}} \quad \text{and} \quad K^{ee} = \frac{K_{12}R_{oo}}{R_{ee}} = \frac{K_{21}R_{oo}}{R_{ee}},$$

where $V^{zt}_{1\to2}$, $V^{zt}_{2\to1}$, V^{ee}, $K^{zt}_{1\to2}$, $K^{zt}_{2\to1}$, $K^{ic}_{1\to2}$, $K^{ic}_{2\to1}$ and K^{ee} represent the velocity and Michaelis constants described in Table 2. The constants of eqn. (1) are related to the mobile carrier rate constants ($a\to h$) in the following way:

$$nR_{12} = \frac{1}{e} + \frac{1}{h} + \frac{1}{c}\left(\frac{e+d}{e}\right),$$

$$nR_{21} = \frac{1}{b} + \frac{1}{g} + \frac{1}{d}\left(\frac{b+c}{b}\right),$$

$$nR_{oo} = \frac{1}{g} + \frac{1}{h}$$

$$nR_{ee} = \frac{1}{b} + \frac{1}{e} + \frac{1}{c}\left(\frac{e+d}{e}\right) + \frac{1}{d}\left(\frac{b+c}{b}\right)$$

$$K_{12} = \frac{bg}{a}\left(\frac{1}{b} + \frac{1}{c}\left(\frac{e+d}{e}\right)\right)$$

$$K_{21} = \frac{eh}{f}\left(\frac{1}{e} + \frac{1}{d}\left(\frac{b+c}{b}\right)\right)$$

with the constraint $bfdg = each$, where n is a constant proportional to the number of carriers. The flux in the opposite direction ($2 \rightarrow 1$; influx) is obtained by interchanging $P \leftrightarrow Q$ and subscripts $1 \leftrightarrow 2$ in eqn. (1).

Using the data shown in Table 2 we can calculate that $R_{12} = 0{\cdot}116$; $R_{21} = 0{\cdot}5$; $R_{ee} = 0{\cdot}5$; $R_{oo} = 0{\cdot}116$; $K_{12} = 5{\cdot}6$; $K_{21} = 5{\cdot}78$ and $K^{ee} = 1{\cdot}32$.

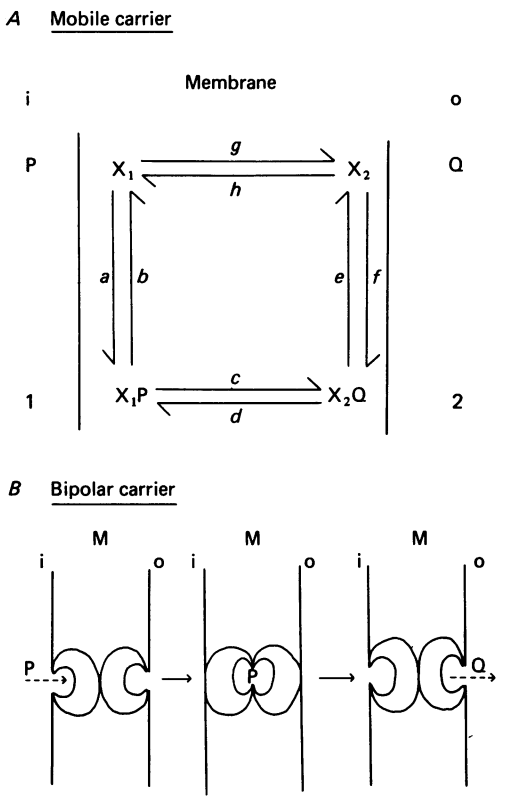

Fig. 3. Models for the transport of sugars in the squid axon. *A*, the mobile carrier. X is carrier, P is sugar on side 1, Q is sugar on side 2. $a \rightarrow h$ are rate constants for the appropriate reactions. *B*, the two-component carrier. The carrier consists of two halves, each of which can bind sugar with a characteristic dissociation constant. When sugar binds, a conformation change occurs, permitting sugar to exchange between each half of the carrier in a central, intramembranous pool. The carrier then undergoes further conformational change releasing the sugar at the opposite side of the membrane. For simplicity the carrier is shown operating in one direction only.

In the Results section, some of the experimental results are fitted with theoretical curves calculated from eqn. (1) using the above values for the constants. The Figure legends indicate where this has been done.

The flux equation for unidirectional exit in the two-component, simultaneous carrier can be derived from Baker & Widdas (1973) as

$$V_{1\to 2}=\left\{\left(\frac{1}{1+\frac{K_1}{P}}\right)\left(1-\left(\frac{1}{1+\frac{K_2}{Q}}\right)\right)\right\}V^{zt}_{1\to 2}+\left\{\left(\frac{1}{1+\frac{K_1}{P}}\right)\left(\frac{1}{1+\frac{K_2}{Q}}\right)\right\}V^{ee} \qquad (2)$$

where $K_1 = K^{zt}_{1\to 2} = K^{ic}_{2\to 1}$; $K_2 = K^{zt}_{2\to 1} = K^{ic}_{1\to 2}$, P and Q refer to the concentrations of sugar at the inside (side 1) and outside (side 2) of the axon respectively. Influx is obtained by interchanging $P \leftrightarrow Q$ and subscripts $1 \leftrightarrow 2$. Table 2 lists the experimental values of K_1 and K_2. Again, some of the experimental results are fitted with theoretical curves calculated from eqn. (2). The Figure legends show where this has been done.

RESULTS

3-O-methylglucose influx

Influx into fibres dialysed with sugar-free medium. The concentration dependence of 3-*O*-methylglucose uptake in three fibres is summarized in Fig. 4. The points can be fitted by a single rectangular hyperbola with an apparent K_m of 1·34 mM and V_{max} of 1·99 pmol . cm^{-2} . s^{-1}. These results compare well with the data from intact fibres where at 21 °C the apparent K_m and V_{max} for uptake are 1·8 mM and 2·3 pmol . cm^{-2} . s^{-1} respectively (Baker & Carruthers, 1981).

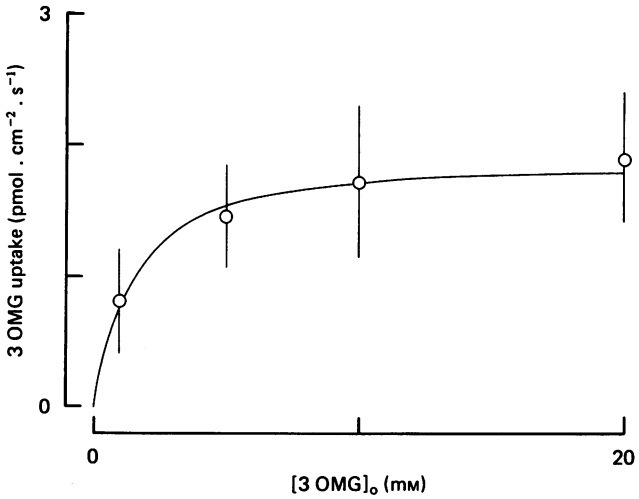

Fig. 4. The dependence of 3-*O*-methylglucose (3 OMG) uptake on sugar concentration Pooled data from three separate experiments. The bars through each point represent ±1 standard error about the mean. Ordinate: 3-*O*-methylglucose uptake in pmol . cm^{-2} . s^{-1}. Abscissa: external 3-*O*-methylglucose concentration (mM). The curve is a rectangular hyperbola with apparent K_m, 1·34 mM and V_{max}, 1·99 pmol . cm^{-2} . s^{-1}. Temperature, 15±1 °C; mean axon diameter, 854 μm; mean E_M, −51·2 mV.

Influx into fibres dialysed with sugar-containing medium. Addition of 3-*O*-methyglucose to the dialysis medium has no measurable effect on the rate of 3-*O*-methylglucose uptake. Fig. 5*A* shows such an experiment where the internal

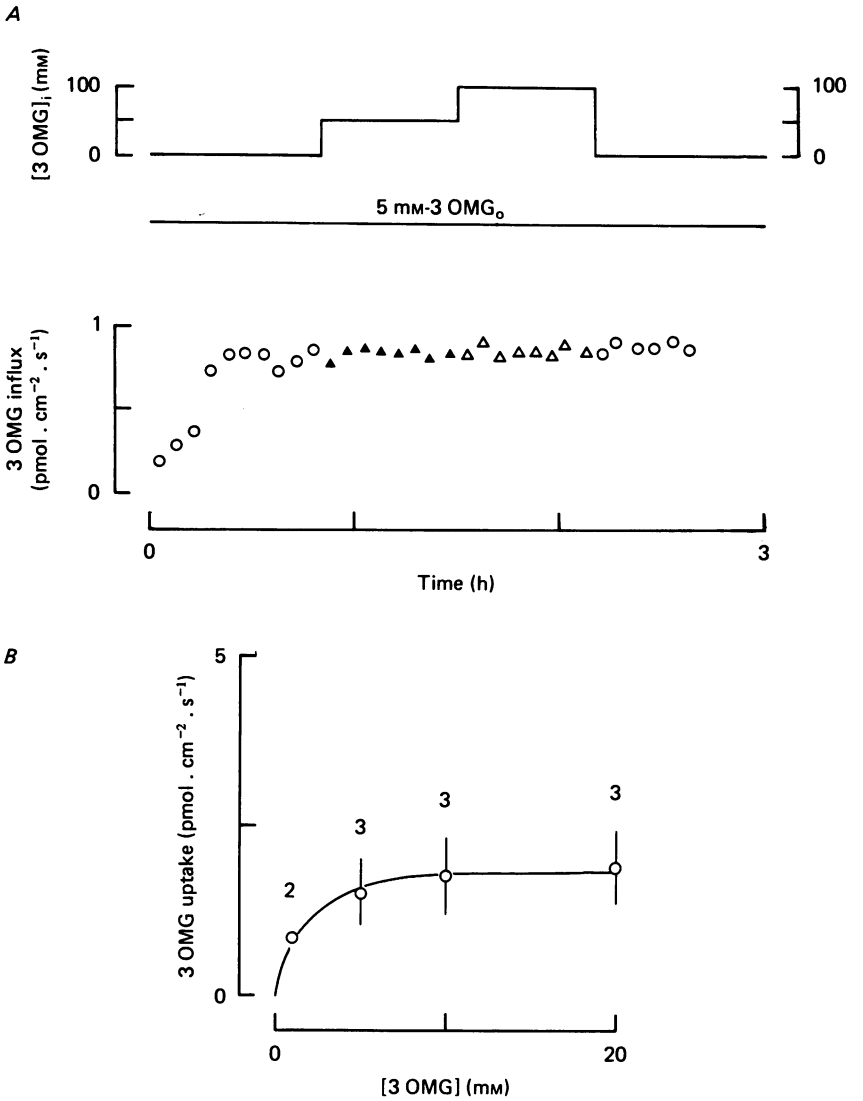

Fig. 5. Effect of intracellular sugar on 3-*O*-methylglucose uptake. *A*, Ordinate: 3-*O*-methylglucose uptake in pmol . cm^{-2} . s^{-1}. Abscissa: time in h. The fibre was dialysed with a solution containing 0, 50 and 100 mM-3-*O*-methylglucose (shown above the points). The external 3-*O*-methylglucose concentration was 5 mM. Temperature, 14 °C; axon diameter, 885 μm; E_M, −52 mV. *B*, equilibrium-exchange influx (internal [sugar] = external [sugar]). Ordinate: 3-*O*-methylglucose uptake in pmol . cm^{-2} . s^{-1}. Abscissa: external and internal sugar concentration (mM). The number of determinations is shown above the points. The curve through the points is a rectangular hyperbola with apparent K_m, 1·35 mM and V_{max}, 1·95 pmol . cm^{-2} . s^{-1}. Temperature, 15 °C; mean axon diameter, 783 μm; mean E_M, −50·9 mV.

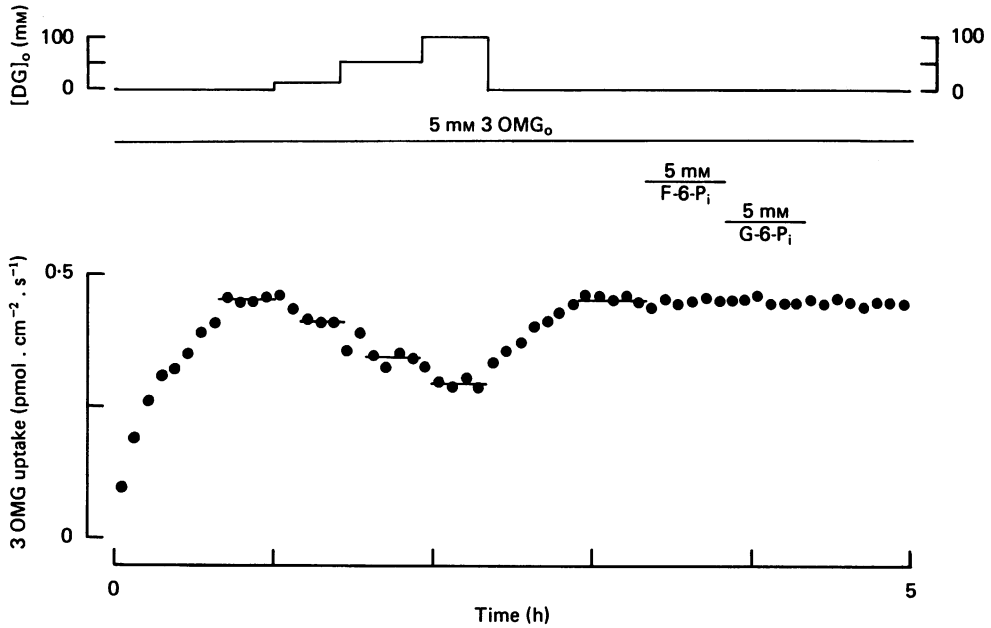

Fig. 6. Effect of external glucose and internal fructose-6-phosphate and glucose-6-phosphate on 3-*O*-methylglucose uptake. Ordinate: 3-*O*-methylglucose uptake in pmol . cm^{-2} . s^{-1}. Abscissa: time in h. The concentration of the various sugars (internal and external) is shown above the points. Temperature, 13 °C; axon diameter, 855 μm; E_M, −53 mV.

A

ATP_i mM	0			5			0
3 OMG_o mM	10	5	15	1	15	5	10

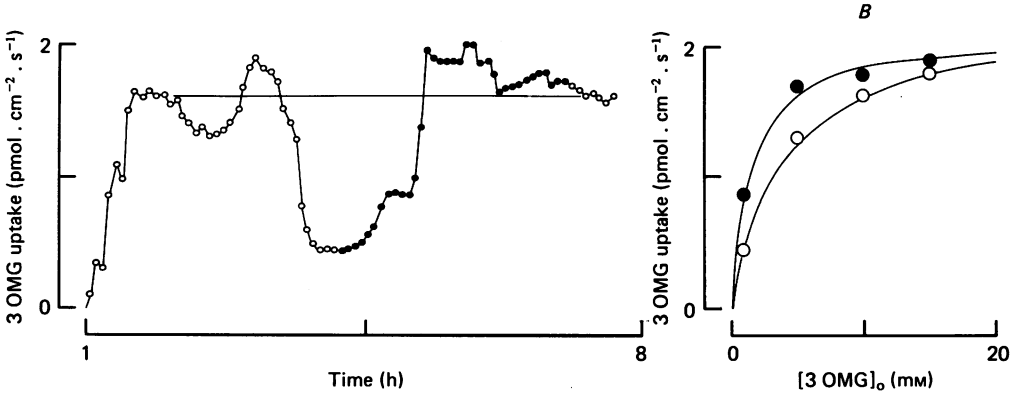

Fig. 7. Effect of ATP_i on kinetics of 3-*O*-methylglucose uptake. *A*, Ordinate: 3-*O*-methylglucose uptake in pmol . cm^{-2} . s^{-1}. Abscissa: time in h. External 3-*O*-methylglucose and internal ATP concentrations are shown above the points. Temperature, 15 °C; axon diameter, 860 μm; E_M, −50 mV. *B*, Figure drawn from *A*. Ordinate: 3-*O*-methylglucose uptake. Abscissa: external 3-*O*-methylglucose concentration (mM). Both curves are rectangular hyperbolae with the following constants; uptake in the presence of 5 mM-ATP_i (-●-): apparent K_m, 1·4 mM; V_{max}, 2·1 pmol . cm^{-2} . s^{-1}; uptake in the absence of ATP_i (-○-): apparent K_m, 4·1 mM; V_{max}, 2·2 pmol . cm^{-2} . s^{-1}.

sugar concentration was raised to 100 mM without causing any detectable change in sugar uptake. Fig. 5*B* summarizes the data from five fibres where 3-*O*-methylglucose uptake was measured under conditions where the external and internal 3-*O*-methylglucose levels were identical (equilibrium-exchange conditions, Lieb & Stein, 1974). The kinetics of equilibrium-exchange uptake are not significantly different from those for uptake in fibres dialysed with sugar-free medium.

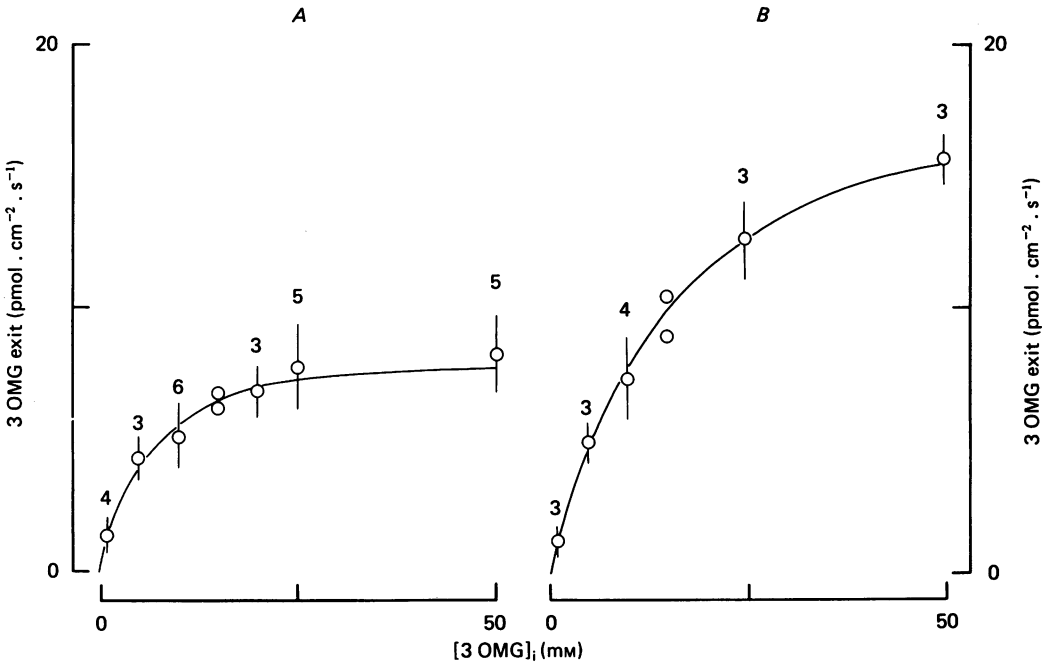

Fig. 8. Concentration-dependence of 3-*O*-methylglucose exit into sugar-free sea water. *A*, exit at 15 °C. Ordinate: 3-*O*-methylglucose exit in pmol . cm^{-2} . s^{-1}. Abscissa: internal 3-*O*-methylglucose concentration (mM). The smooth curve is a rectangular hyperbola with apparent K_m, 5·5 mM and V_{max}, 8·6 pmol . cm^{-2} . s^{-1}. Mean axon diameter, 694 μm; mean E_M, −532 mV. *B*, exit at 21 °C. Ordinate: 3-*O*-methylglucose efflux. Abscissa: internal 3-*O*-methylglucose concentration. The curve is a rectangular hyperbola with apparent K_m, 15·6 mM and V_{max}, 20·2 pmol . cm^{-2} . s^{-1}. Mean temperature, 21 ± 1 °C; mean axon diameter, 755 μm; mean E_M, −52·5 mV. The number of measurements is shown above the points.

In a number of experiments the effects of internal sugars on the rate of D-glucose or 2-deoxy-D-glucose uptake were examined. The results showed that in all cases sugar uptake was unaffected by the presence of intracellular sugar. Fig. 6 shows that addition of products of glucose metabolism (glucose-6-phosphate and fructose-6-phosphate) to the dialysis medium are also without effect on 3-*O*-methylglucose uptake.

Competition between sugars for uptake. Raising external D-glucose levels from 0 to 100 mM in sea water containing 5 mM-3-*O*-methylglucose progressively reduces the rate of 3-*O*-methylglucose uptake (Fig. 6). Conversely, D-glucose uptake in dialysed fibres superfused with artificial sea water (ASW) containing 20 mM-glucose is reduced by 50 % on addition of 20 mM-3-*O*-methylglucose to the external solution.

Effect of ATP_i on the kinetics of 3-O-methylglucose uptake. When fibres are dialysed with ATP-free medium, the kinetics of sugar uptake are altered (see Fig. 7): the V_{max}

for uptake in the absence of ATP_i appears to be unchanged; but the apparent K_m for uptake of 3-*O*-methylglucose is increased from 1·4 to 4·1 mM.

3-O-methylglucose efflux

Efflux into sugar-free sea water. The kinetics of 3-*O*-methylglucose exit in squid axons are extremely sensitive to changes in temperature. Fig. 8(*A*, *B*) illustrates this point. The concentration dependence of exit at 15 °C is shown in Fig. 8*A*. The relationship between exit and sugar concentration can be approximated by a single

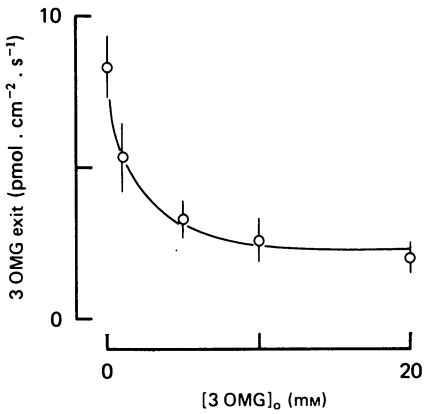

Fig. 9. Effect of extracellular 3-*O*-methylglucose on 3-*O*-methylglucose exit. Ordinate: 3-*O*-methylglucose exit in pmol . cm^{-2} . s^{-1}. Abscissa: extracellular 3-*O*-methylglucose concentration (mM). Data pooled from six separate experiments. Each fibre was dialysed with medium containing 50 mM-3-*O*-methylglucose. The smooth curve is calculated from eqns. (1) and (2) of the Methods section. Mean axon diameter, 782 μm; mean E_M, −50·4 mV.

rectangular hyperbola with an apparent K_m of 5·5 mM and V_{max} of 8·6 pmol . cm^{-2} . s^{-1}. At 21 °C, however, the kinetics of exit are markedly different (Fig. 8*B*). Although the data are less complete the relationship between efflux and sugar concentration can again be approximated by a single rectangular hyperbola with apparent K_m of 15·6 mM and V_{max} of 20·2 pmol . cm^{-2} . s^{-1}. The Q_{10} for 3-*O*-methylglucose exit in the dialysed axon (50 mM internal 3-*O*-methylglucose) between 21 and 15 °C is 3·3 which is in close agreement with the Q_{10} for exit in the intact axon over the same temperature range (3·2; see Baker & Carruthers, 1981).

Efflux of 3-O-methylglucose into sea water containing 3-O-methylglucose. As in the intact axon, (Baker & Carruthers, 1981) the efflux of 3-*O*-methylglucose in dialysed axons is reduced on addition of sugar to the external medium. The reduction in sugar exit by external 3-*O*-methylglucose appears to be unrelated to the internal 3-*O*-methylglucose concentration (range 1–100 mM) but is critically dependent on the external sugar concentration. Fig. 9 summarizes the dependence of this inhibition of 3-*O*-methylglucose exit on the external 3-*O*-methylglucose concentration. In each fibre the internal 3-*O*-methylglucose concentration was 50 mM at which concentration the internal sugar binding sites are 90 % saturated with sugar. The concentration of 3-*O*-methylglucose which reduces sugar efflux half-maximally is 1·8 mM which is close to the apparent K_m for 3-*O*-methylglucose uptake in squid axons.

Fig. 10(*A*, *B*) shows the effect of 5 mM external 3-*O*-methylglucose on the kinetics

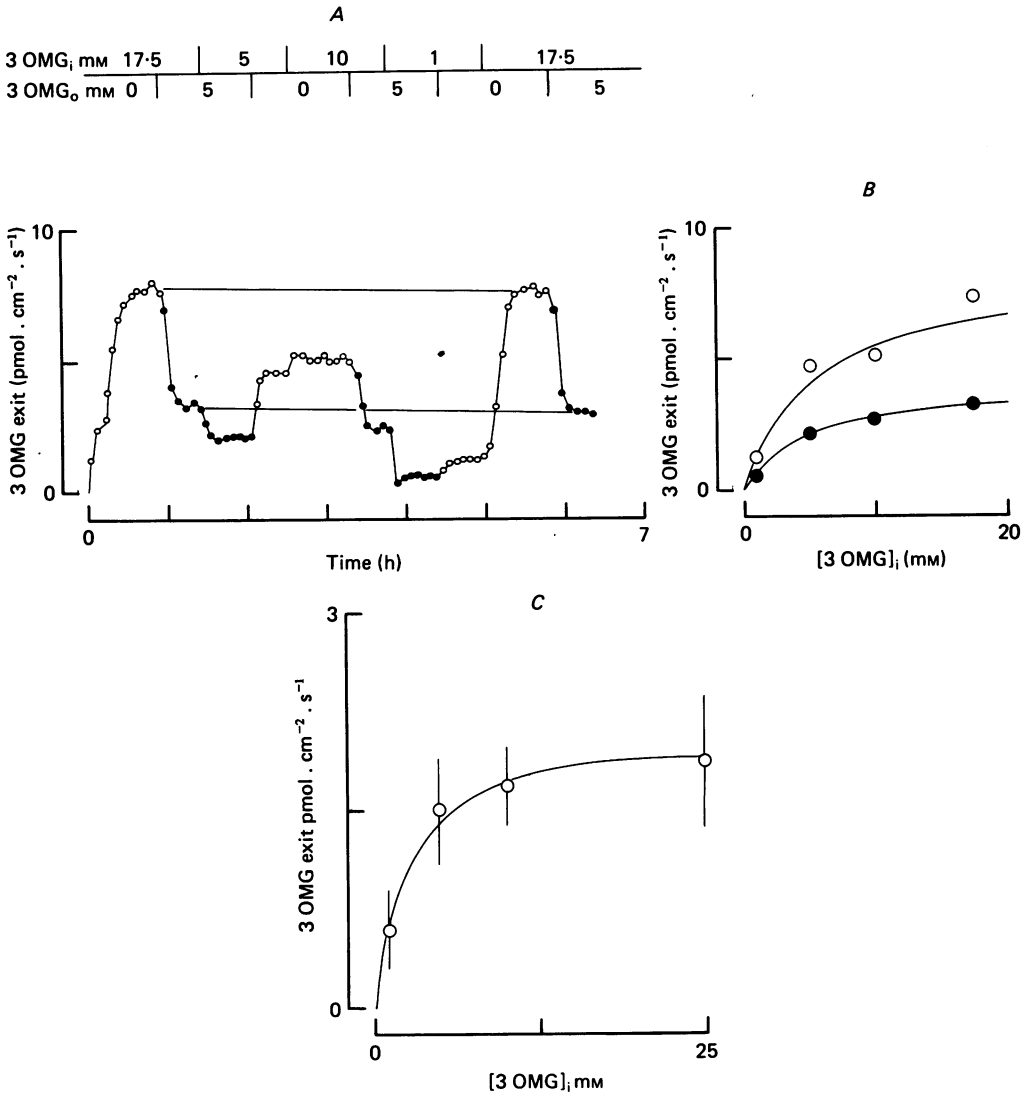

Fig. 10. Effect of extracellular 3-*O*-methylglucose on kinetics of 3-*O*-methylglucose exit. *A*, concentration dependence of 3-*O*-methylglucose exit in the absence and presence of 5 mM external 3-*O*-methylglucose. Ordinate: 3-*O*-methylglucose exit in pmol . cm^{-2} . s^{-1}. Abscissa: time in h. External and internal sugar concentrations are shown above the points. Temperature, 15 °C; axon diameter, 825 μm; E_M, −56 mV. *B*, Figure redrawn from *A*. Ordinate: 3-*O*-methylglucose exit. Abscissa: internal 3-*O*-methylglucose concentration (mM). Both smooth curves are calculated from eqns. (1) and (2) of the Methods section. Open circles, control sugar exit into sugar-free solution. Filled circles, exit in the presence of 5 mM-3-*O*-methylglucose. *C*, 3-*O*-methylglucose efflux under conditions of equilibrium-exchange. Data pooled from six separate experiments. The curve is a section of a rectangular hyperbola with apparent K_m, 1·45 mM and V_{max}, 2·1 pmol . cm^{-1} . s^{-1}. Mean temperature, 15 °C; mean axon diameter, 720 μm; mean E_M, −50·1 mV.

of 3-*O*-methylglucose efflux. The apparent K_m for exit seems to be unaltered by the presence of extracellular sugar but the V_{max} for efflux is reduced almost three-fold from 8·1 to 3·5 pmol . cm^{-2} . s^{-1}. The concentration dependence of 3-*O*-methylglucose exit under conditions of equilibrium exchange (internal [sugar] equals external [sugar]) is shown in Fig. 10*C*. Here the kinetics of exit are close to the kinetics of uptake under the same conditions (see Fig. 5*B*).

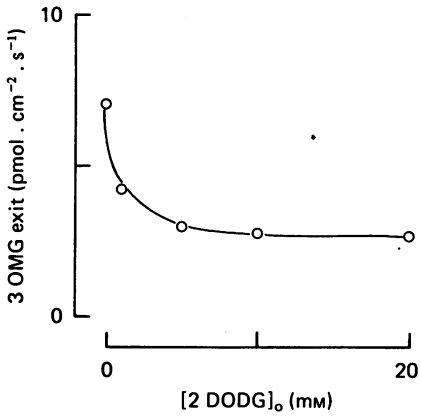

Fig. 11. Effect of extracellular 2-deoxy-D-glucose on 3-*O*-methylglucose exit. Ordinate: 3-*O*-methylglucose efflux in pmol . cm^{-2} . s^{-1}. Abscissa: external 2-deoxy-D-glucose concentration (mM). The fibre was dialysed with a solution containing 50 mM-3-*O*-methylglucose. Temperature, 15 °C; axon diameter, 745 μm; E_M, −53 mV.

The asymmetry in sensitivity of 3-*O*-methylglucose exit and uptake to the presence of sugar at the opposite, *trans* side of the membrane might arise because of the difference in the composition of extracellular and dialysis solutions. This possibility was tested by measuring the response of the sugar efflux system to external sugar under conditions where the ionic composition of the solution on both sides of the membrane was identical. This was achieved by replacing sea water with dialysis medium. External 3-*O*-methylglucose still reduces sugar exit when sea water is replaced by dialysis fluid although the absolute rate of 3-*O*-methylglucose exit is increased five-fold. Sugar efflux recovers rapidly on replacing the external dialysate with sea water but membrane potential does not show full recovery following the period of complete depolarization. The increased sugar exit and low final membrane potential may be caused by the low divalent cation levels to which the exterior of the fibre has been exposed for up to 1½ h. The opposite condition where internal dialysis fluid is replaced with sea water was not examined. This observation suggests that the origin of the asymmetry resides in the membrane and not in the solutions bathing it.

Efflux into sea water containing D-glucose and 2-deoxy-D-glucose. Extracellular 2-deoxy-D-glucose reduces the rate of 3-*O*-methylglucose efflux. Fig. 11 summarizes the effect of 2-deoxy-D-glucose on efflux in a fibre dialysed with 50 mM-3-*O*-methylglucose. The concentration of external 2-deoxy-D-glucose which reduces sugar exit half-maximally in the dialysed axon (0·8 mM) is close to the Michaelis constant for inhibition of exit in the intact axon (0·59 mM).

The effect of external D-glucose on 3-*O*-methylglucose efflux is more complex (see Fig. 12*A*). In Na-free choline ASW, external glucose reduces the rate of 3-*O*-methylglucose exit. In full Na ASW, however, glucose stimulates 3-*O*-methylglucose efflux. The magnitude of the effects of glucose on 3-*O*-methylglucose exit in Na-free and Na ASW is not always as large as those shown in Fig. 12*A* but the results are essentially similar. In fibres dialysed with 50 mM-3-*O*-methylglucose, external glucose

(20 mM) in Na ASW increases the rate of exit 1·45-fold ($n = 4$). This represents an increase in exit of about 3·5 pmol.cm^{-2}.s^{-1} from 8 to 11·5 pmol.cm^{-2}.s^{-1} in Na ASW. The variability of the effects of glucose on exit into Na ASW probably reflects the inherent variability of the transport properties of individual axons. Fig. 12*B* summarizes the effect of D-glucose on 3-*O*-methylglucose exit into Na-free choline

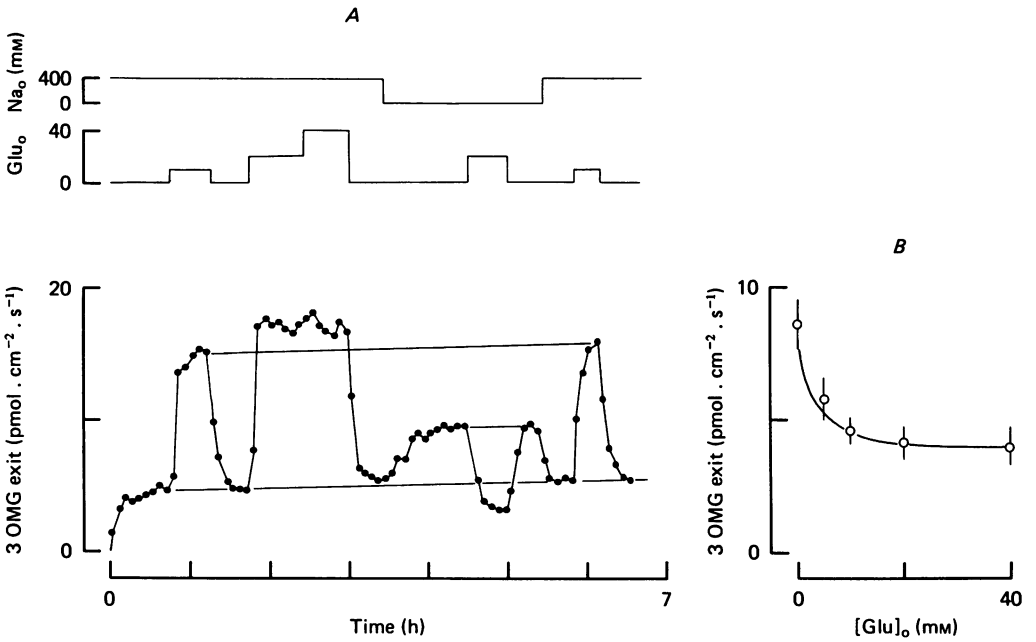

Fig. 12. Effect of extracellular glucose on 3-*O*-methylglucose exit. *A*, effect in NaASW and Na-free (choline) ASW. Ordinate: 3-*O*-methylglucose exit in pmol.cm^{-2}.s^{-1}. Abscissa: time in h. Internal 3-*O*-methylglucose concentration = 50 mM. External glucose and Na concentrations are shown above the points. Temperature, 15 °C; axon diameter, 823 μm; E_M, −56 mV. *B*, 3-*O*-methylglucose efflux into Na-free ASW containing glucose. Ordinate: 3-*O*-methylglucose efflux. Abscissa: extracellular glucose concentration (mM). The data are pooled from three separate experiments and each fibre was dialysed with a solution containing 50 mM-3-*O*-methylglucose. The smooth curve is an inverted section of a rectangular hyperbola with apparent K_i for external glucose, 3·2 mM and maximum inhibition 50%. Mean temperature, 15 °C; mean axon diameter, 785 μm: mean E_M, −50·8 mV.

ASW. In both Na and Na-free ASW the apparent K_m of the external site for glucose is 3–3·5 mM which is close to the apparent K_m for glucose uptake in intact axons.

Competition between internal sugars for exit. Fig. 13 summarizes the effects of a variety of internal sugars on 3-*O*-methylglucose efflux. In fibres dialysed with a constant concentration of 3-*O*-methylglucose, addition of increasing concentrations of D-glucose to the dialysis medium progressively reduces the rate of 3-*O*-methylglucose efflux. 3-*O*-Methylglucose efflux falls when 50 mM-D-glucose is added to the internal solution but increases as the concentration of 3-*O*-methylglucose is raised in the presence of D-glucose. This is good evidence for competition between D-glucose and 3-*O*-methylglucose for exit. α-Methyl-D-glucopyranoside (50 mM) reduces the rate of 3-*O*-methylglucose efflux much less than 50 mM-D-glucose or 50 mM-2-deoxy-D-

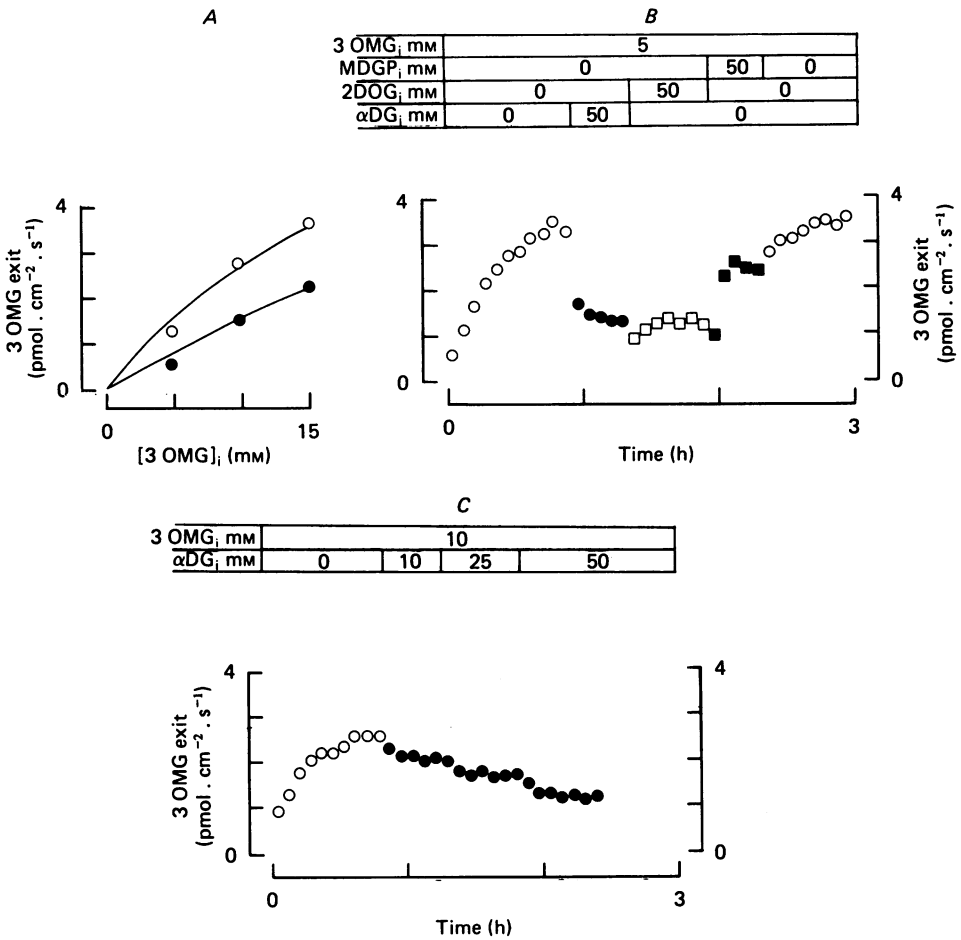

Fig. 13. Competition between sugars for exit. *A*, effect of 50 mM internal glucose on 3-*O*-methylglucose efflux. Ordinate: 3-*O*-methylglucose efflux in pmol . cm^{-2} . s^{-1}. Abscissa: internal 3-*O*-methylglucose concentration (mM). Efflux is shown in the absence (–○–) and presence (–●–) of 50 mM internal glucose. This Figure summarizes a single experiment. Temperature, 14 °C; axon diameter, 1082 μm; E_M, −51 mV. *B*, the effect of different internal sugars on 3-*O*-methylglucose efflux. Ordinate: 3-*O*-methylglucose efflux. Abscissa: time in h. The fibre was dialysed with a solution containing 5 mM-3-*O*-methylglucose. The times at which 50 mM-glucose, 2-deoxy-D-glucose and α-methyl-D-glucopyranoside were added to the internal solution are shown above the points. Temperature, 14 °C; axon diameter, 760 μm; E_M, −56 mV. *C*, the effects of increasing internal glucose levels on the rate of 3-*O*-methylglucose efflux. Ordinate and abscissa as in *B*. The fibre was dialysed with a solution containing 10 mM-3-*O*-methylglucose and the D-glucose content of the solution was raised progressively from 0 to 50 mM. Temperature, 15 °C; axon diameter, 988 μm; E_M, −50 mV.

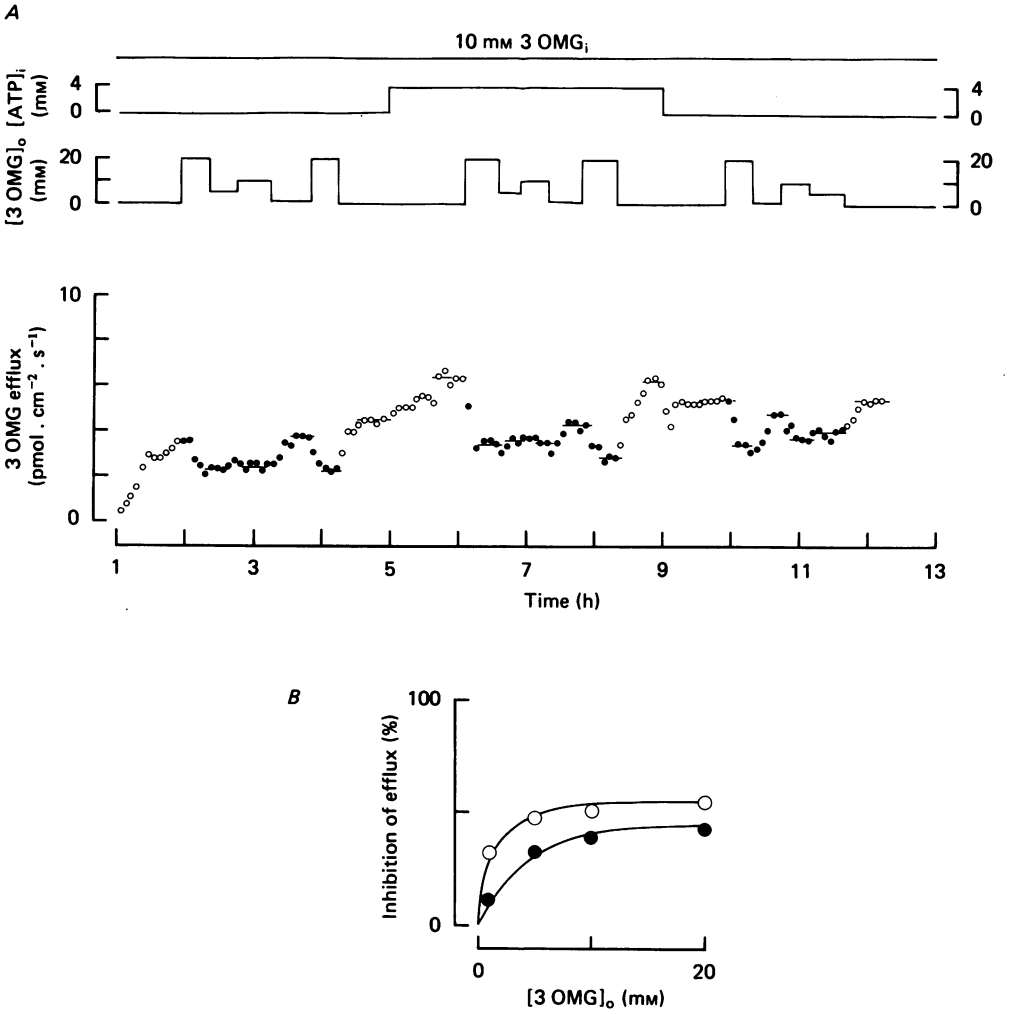

Fig. 14. Effect of external 3-*O*-methylglucose on 3-*O*-methylglucose exit in a fibre dialysed with medium containing 4 mM- and zero-ATP. *A*, Ordinate: 3-*O*-methylglucose efflux in pmol . cm^{-2} . s^{-1}. Abscissa: time in h. The concentrations of 3-*O*-methylglucose and ATP in the dialysate and external 3-*O*-methylglucose are shown above the points. The fibre was dialysed with zero-ATP medium for 1 h before the radioactive sugar was added. Temperature, 14 °C; axon diameter, 760 μm; E_M at $t = 0$ h, −53 mV; E_M at $t = 13$ h, −37 mV. *B*, Redrawn from *A*. Ordinate: % reduction in 3-*O*-methylglucose exit by extracellular sugar. Abscissa: external 3-*O*-methylglucose concentration (mM). Both curves are rectangular hyperbolae with the following constants; 4 mM-ATP in dialysate (–○–): apparent K_m for inhibition of exit by external sugars, 0·72 mM; maximum inhibition, 54·3%. Zero-ATP in dialysate (–●–): apparent K_m for inhibition of exit by external sugar, 3·22 mM; maximum inhibition, 55·5%.

glucose, suggesting that the internal sugar transport site is stereospecific. The apparent K_i for the competitive inhibition of 3-*O*-methylglucose exit by glucose, 2-deoxy-D-glucose and α-methyl-D-glucopyranoside are $11{\cdot}5 \pm 1{\cdot}2$ mM ($n = 5$), $6{\cdot}9 \pm 1{\cdot}7$ mM ($n = 3$) and 28·3 mM ($n = 2$) respectively.

ATP_i and 3-O-methylglucose efflux. After dialysis with an ATP-free solution for 4 h the efflux of 3-*O*-methylglucose is reduced by approximately 33%. This effect is reversed by adding 4 mM-ATP to the dialysis solution (see Fig. 14). In the nominal absence of ATP_i, the concentration of external 3-*O*-methylglucose which reduces sugar efflux half-maximally is 3·2 mM. When 4 mM-ATP is added to the dialysis medium, half-maximal inhibition of exit is produced by 0·72 mM external 3-*O*-

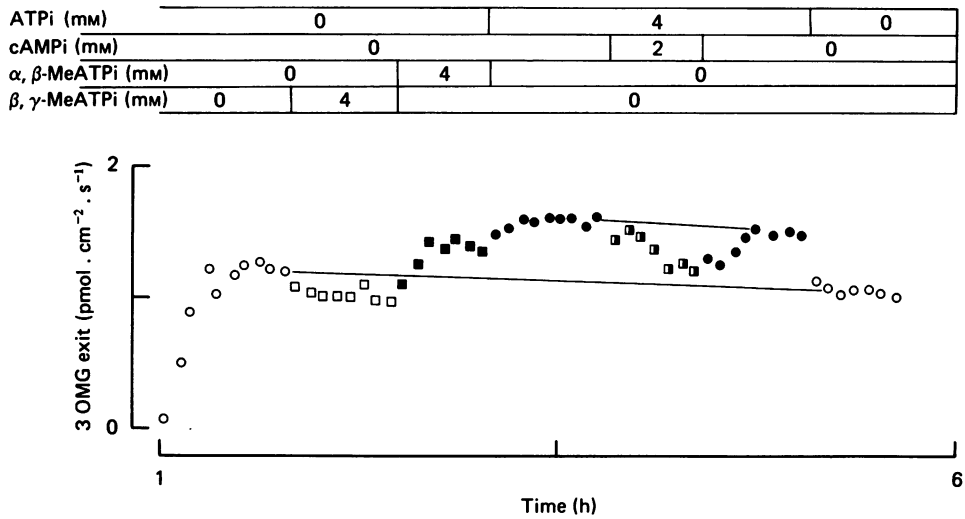

Fig. 15. Effects of analogues of ATP on 3-*O*-methylglucose exit. Ordinate: 3-*O*-methylglucose efflux in pmol . cm^{-2} . s^{-1}. Abscissa: time in h. The fibre was dialysed with ATP-free medium containing 5 mM-3-*O*-methylglucose for 1 h before isotope was added. The various analogues of ATP and other nucleotides were added to the internal solution at different times during the experiment (see key above points). Temperature, 15 °C; axon diameter, 690 μm.

methylglucose but the maximum inhibition remains unchanged (55·1%). These data resemble those for the effects of ATP_i on uptake where the apparent K_m for uptake is increased in the nominal absence of ATP_i but the maximum velocity of uptake is unchanged.

In the nominal absence of ATP_i, internal application of 2 mM-AMP, 2 mM-ADP and 2 mM-GTP are without effect on the rate of 3-*O*-methylglucose exit (5 mM internal 3-*O*-methylglucose). However, the hydrolysable analogue of ATP (α, β-methylene-5-ATP, 4 mM) but not the non-hydrolysable analogue (β, γ-methylene-5-ATP, 4 mM) increases the rate of 3-*O*-methylglucose exit in the nominal absence of ATP_i (Fig. 15). In the presence of 4 mM-ATP_i, internal application of cyclic AMP (2 mM) produces a small and reversible decrease in the rate of sugar exit (see Fig. 15) but lower concentrations of cyclic AMP (μM range) are without effect on exit.

Low, but physiological, intracellular levels of glucose-6-phosphate (0·03 mM),

glucose-1-phosphate (0·01 mM), fructose-6-phosphate (0·01 mM) or lactate (0·13 mM) (Storey & Storey, 1978) have no measurable effect on 3-*O*-methylglucose efflux in dialysed fibres. Raising internal free Ca from 0·04 to 0·9 μM is also without effect on the rate of sugar efflux in fibres dialysed with solution containing 4 mM-ATP, pH 7·2. 3-*O*-Methylglucose efflux, however, is reduced by some 20% when the pH of the dialysis medium is lowered from 7·2 to 6·0 (ATP_i = 4 mM; ionized [Ca] = 0·01–0·1 μM).

TABLE 1. Comparison of 3-*O*-methylglucose transport in dialysed and intact axons*

	Dialysed axon	*Intact axon*
Uptake		
Apparent K_m	1·34 mM	1·78 mM
V_{max}	1·99 pmol . cm^{-2} . s^{-1}	2·33 pmol . cm^{-2} . s^{-1}
ATP depletion	Reduces uptake	Reduces uptake†
	Reduces exit	Reduces exit
Internal acidification	Reduces exit	Reduces exit
Q_{10} exit (21–15 °C)	3·3	3·2
Effects of external sugars on exit	Reduces exit. Inhibition by 3-*O*-methylglucose > 2-deoxyglucose > D-glucose	Reduces exit. Inhibition by 3-*O*-methylglucose > 2-deoxyglucose > D-glucose
Concentration which produces half-maximal reduction in exit		
3-*O*-methylglucose	1·78 mM	1·85 mM
2-deoxyglucose	0·79 mM	0·67 mM
D-glucose	3·25 mM	3·6 mM‡

* Unless stated dialysis medium contained 4 mM-ATP, pH 7·2.
† Glucose uptake.
‡ Intact fibre injected to give final internal concentration of 3-*O*-methylglucose of 50 mM.

DISCUSSION

Comparison with intact axons

Transport studies in single cells are simplified considerably if it is possible to control the concentration of solutes on both sides of the membrane. In this paper we have characterized the transport of the non-metabolized sugar 3-*O*-methylglucose in squid axons where the intracellular environment of the cell is controlled by internal dialysis. There is, of course, no *a priori* reason to assume that the transport properties of the axolemma will be unaffected by dialysis, but a comparison of the properties of sugar transport in dialysed and intact axons shows close agreement (see Table 1).

Characteristics of 3-O-methylglucose transport in squid axons

Despite the fact that the squid axon does not accumulate 3-*O*-methylglucose (see Baker & Carruthers, 1981), under zero-trans conditions when sugar is present on one side of the membrane only the kinetics of 3-*O*-methylglucose uptake and exit exhibits marked asymmetry. At 15 °C, the apparent K_m and V_{max} for exit are some 4·4 times those for uptake. The squid axon is not unique in this respect. Sugar transport in the human red cell is passive and asymmetric with the apparent K_m and V_{max} for exit some 10 times those for uptake (see Naftalin & Holman, 1977; Widdas, 1980). However, there are some important differences in the way that the squid axon and the human red cell transport sugars. In the human red cell, both glucose uptake and exit are increased when glucose is present at the opposite, *trans*-side of the membrane

(Rosenberg & Wilbrandt, 1957; Miller, 1968). In the squid axon, sugar exit is reduced by external sugar and uptake is unaffected by axoplasmic sugar. Thus, under conditions where internal and external activities of sugar are equal and no net transfer of sugar is possible, so-called equilibrium-exchange, the kinetics of glucose uptake and exit in the human red cell are altered in such a way that the V_{max} for unidirectional exchange fluxes is greater than the V_{max} for uptake or exit in the absence of *trans*-sugars. In the squid axon, however, only the kinetics of sugar exit are changed under equilibrium-exchange conditions becoming identical to the kinetics of uptake. It seems that, whereas both uptake and exit in the red cell are sensitive to *trans*-sugar, the kinetics of uptake in the squid axon are invariant and, under exchange conditions, determine the kinetics of sugar exit.

Another interesting difference between transport in the human red cell and squid axon is the sensitivity of transport to temperature. In the human red cell, the Q_{20} for influx between 0 and 20 °C is 170 (Lacko, Wittke & Kromphardt, 1972) whereas the exit data of Sen & Widdas (1962) are consistent with a Q_{10} for exit between 7 and 17 °C of 4. These results suggest that the asymmetry between the V_{max} for net influx and efflux is increased as the temperature is lowered from 15 to 5 °C. The reverse phenomenon is observed in the squid axon. The Q_{15} for glucose uptake between 0 and 15 °C is 1·9 and that for 3-*O*-methylglucose exit over the same temperature range is 7·8 (see Baker & Carruthers, 1981). These results suggest that the asymmetry between V_{max} for exit and influx is reduced as the temperature is lowered. Consistent with this view is the finding that asymmetry between V_{max} for exit and uptake at 21 °C in the squid axon is 9 (using intact axon data for uptake (Baker & Carruthers, 1981) and dialysed axon data for exit) and at 15 °C the asymmetry between V_{max} for exit and entry is 4·4.

Effect of external trans-sugars on 3-O-methylglucose exit

An important feature of sugar fluxes in red cells is their acceleration by *trans*-sugars: a phenomenon known as 'the substrate-facilitated transfer of the glucose carrier across the human erythrocyte membrane' (Levine, Oxender & Stein, 1965). With only one exception, stimulation of 3-*O*-methylglucose fluxes by *trans*-sugar is not observed in squid axons. Unidirectional sugar uptake is unaffected by internal sugar and unidirectional sugar exit is reduced by external sugar. The single exception is the stimulation of sugar exit by external D-glucose in NaASW. In choline (Na-free) ASW, external D-glucose reduces 3-*O*-methylglucose exit.

Three possible explanations for the inhibition of 3-*O*-methylglucose exit by external sugar are: transport along a long pore; the existence of unstirred layers at the inner surface of the membrane; or a property of the transport system itself.

The reduction in unidirectional sugar exit by external sugar is unlikely to be due to a long-pore effect (Hodgkin & Keynes, 1955) because internal sugar has no effect on sugar uptake. The existence of unstirred layers seems more likely. According to this view, inhibition of sugar exit by external sugar is brought about because the influx of non-radioactive sugar may reduce the specific activity of the radioactive sugar in the microenvironment of the efflux transport sites. This seems unlikely for a number of reasons.

(*a*) The *trans* effect of external sugar persists when the fibre is dialysed with internal sugar concentrations as high as 100 mM.

(*b*) In Na sea water D-glucose promotes a sustained increase in the rate of 3-*O*-methylglucose efflux whereas in Na-free sea water glucose reduces 3-*O*-methylglucose exit. As D-glucose uptake in Na ASW is greater than in choline ASW

(Baker & Carruthers, 1981), unstirred layer effects should be greater when the effects of *trans*-glucose are measured in NaASW.

These results suggest that the inhibition of sugar exit by external sugar does not result from factors extrinsic to the membrane and is a property of the transport system itself.

The simplest kinetic treatments of the facilitated transfer of sugars across cell membranes have usually been based on a symmetrical carrier transfer mechanism (Lefevre, 1948; Widdas, 1952). In the human red cell, however, a number of kinetic anomalies such as asymmetric transport have been reported which have been interpreted in a variety of ways ranging from differences in the membrane mobility of saturated and unsaturated carriers (Britton, 1957; Mawe & Hempling, 1965) to the need to postulate a protein tetramer with four glucose binding sites (Lieb & Stein, 1970). Either of these hypotheses can give rise to more complex kinetics based on a symmetrical mechanism of transport. However, Regen & Morgan (1964) and Geck (1971) have shown that the essential kinetic characteristics of sugar transport in red cells can be given by an asymmetric mobile-carrier system (see Fig. 3*A*). Essentially, the mobile carrier is a single component carrier which is only alternately in contact with the solutions bathing either side of the membrane. Thus only one sugar molecule may be bound by the carrier at any time. That there may be more fundamental asymmetry in red cell sugar transport has been suggested by Wilbrandt (1954) and Baker & Widdas (1973). Baker & Widdas (1973) considered that transport in the red cell may take place by a two-component (or simultaneous) carrier system where sugar binding sites exist simultaneously at each side of the membrane (see Fig. 3*B*). Thus the carrier system can bind two molecules of sugar simultaneously, the inside with a higher K_m than the outside.

The kinetic flux equations for both the mobile-carrier and two-component-carrier models have been excellently reviewed by Lieb & Stein (1974), Britton (1964), Bowyer & Widdas (1958) and Baker & Widdas (1973). Using the data for 3-*O*-methylglucose transport in the dialysed squid axon (see Table 2) it can be shown readily that transport in the squid nerve is consistent both with the asymmetric mobile-carrier and the two-component asymmetric carrier models. It is not possible to distinguish between the two models using the available data.

With the mobile carrier there are four rate constants to consider, g, h, c, and d (see Fig. 3*A*). If the rate of return of loaded carrier from outside to inside is slower than the rate of return of empty carrier to the inside (i.e. $d < h$), then, provided loaded and empty carrier move equally rapidly from inside to outside but at the same rate as unloaded carrier returns to the inside (i.e. $c = h = g > d$) there will be a redistribution of carrier at the outside. This redistribution of carriers can be assessed using eqns. (12) and (13) and (20) and (21) of Widdas (1952). Our data suggest that in the absence of external sugar, carrier is equally distributed between both sides of the membrane but under conditions of saturating concentrations of sugar at both sides of the membrane $\frac{7}{8}$ of the carrier must be at the outer face of the membrane and only $\frac{1}{8}$ at the inner face. Thus external sugar reduces the rate of sugar exit but internal sugar is without effect on uptake. As the asymmetry increases with temperature, this should be reflected in an even more marked redistribution of carriers. In much the same way using the simultaneous model for transport, the corresponding intramolecular change which transfers the system from an outward facing to an inward facing mode (see Fig. 3*B*) may be presumed to be slower when sugar occupies the external binding site.

TABLE 2. Kinetics of 3-*O*-methylglucose transport in the dialysed squid axon

Type of experiment	Conditions	Characterized by	Measured values†
	Blood [sugar] / Axoplasm [sugar]		
Zero-*trans* fluxes			
Uptake	varied / zero	K_m uptake ($K^{si}_{2\to1}$)	1·34 mM
		V_{max} uptake ($V^{si}_{2\to1}$)	1·99 pmol.cm^{-2}.s^{-1}
Exit	zero / varied	K_m exit ($K^{si}_{1\to2}$)	5·5 mM
		V_{max} exit ($V^{si}_{1\to2}$)	8·6 pmol.cm^{-2}.s^{-1}
Infinite-*trans* fluxes			
Uptake	varied / saturating	K_m external ($K^{ti}_{2\to1}$)	1·34 mM
		V_{max} exchange (V^{ee})	1·99 pmol.cm^{-2}.s^{-1}
Exit	saturating / varied	K_m internal ($K^{ti}_{1\to2}$)	5·5 mM
		V_{max} exchange (V^{ee})	2·1 pmol.cm^{-2}.s^{-1}
Infinite-*cis* fluxes*			
Uptake	saturating / varied	K_m internal ($K^{ic}_{2\to1}$)	6·0 mM
		V_{max} net entry ($V^{si}_{2\to1}$)	2·2 pmol.cm^{-2}.s^{-1}
Exit	varied / saturating	K_m external ($K^{ic}_{1\to2}$)	1·34 mM
		V_{max} net exit ($V^{si}_{1\to2}$)	8·6 pmol.cm^{-2}.s^{-1}
Equilibrium-exchange			
Internal [sugar] = external [sugar] uptake and exit	varied / varied	K_m exchange (K^{ee})	1·39 mM
		V_{max} exchange (V^{ee})	2·0 pmol.cm^{-2}.s^{-1}

* Infinite-*cis* net fluxes were measured as the difference between unidirectional uptake and exit.

† Obtained by Lineweaver–Burk analysis of experimental data.

Internal ATP and sugar transport

The kinetics of 3-*O*-methylglucose transport are altered when internal ATP levels are reduced close to zero. The interaction of ATP with the transport system seems to increase the affinity of the system for sugar. An analysis of the kinetics of zero *trans*-3-*O*-methylglucose uptake in the presence and nominal absence of ATP_i shows that the apparent K_m for uptake is increased when ATP_i is lowered. The V_{max} for uptake is unchanged. This is also shown in the altered kinetics for the inhibition of sugar efflux by external sugar. The naturally occurring nucleotides AMP, ADP, GTP and cyclic AMP cannot substitute for ATP in this action.

ATP also increases the affinity of the glutamate transport system for its substrate in invertebrate nerve (Baker & Potashner, 1973) although it is not known whether this involves hydrolysis of ATP. The hydrolysable analogue of ATP (α, β-methylene-5-ATP) increases the rate of sugar exit in the nominal absence of ATP_i. Interestingly, the non-hydrolysable analogue, β, γ-methylene-5-ATP, does not share this ability and, if anything, reduces the rate of sugar exit. It is possible that the non-hydrolysable analogue binds to the ATP binding site but is unable to donate a phosphate group. The analogue, therefore, may compete with any endogenous ATP remaining in the axon and reduce phosphorylation of the regulatory site(s) by ATP. This type of effect has been described in squid axons for ATP-dependent uncoupled Ca extrusion (Di Polo, 1977).

These effects of ATP on the transport of sugars in the squid axon can be described by the model shown below:

$$\begin{array}{ccccc} C+S & \overset{K_1}{\rightleftharpoons} & C.S & \xrightarrow{V_1} & \\ + & & + & & \\ ATP & & ATP & & \\ \uparrow{\scriptstyle K_2} & & \uparrow{\scriptstyle K_4} & & \\ C.ATP+S & \overset{K_3}{\rightleftharpoons} & C.ATP.S & \xrightarrow{V_2} & \end{array}$$

where C is carrier, S is sugar, C.ATP is the product of interaction of the transport carrier with ATP, K_1, K_2, K_3 and K_4 are dissociation constants and V_1 and V_2 are rate constants proportional to the rate of transfer of sugar across the axolemma. Making the assumption that all reactions are rapid with respect to V_1 and V_2 it can be shown that

$$\frac{J}{T} = \frac{V_1\frac{[S]}{K_1} + V_2\frac{[S][ATP]}{K_2K_3}}{1+\frac{[S]}{K_1}+\frac{[ATP]}{K_2}+\frac{[S][ATP]}{K_2K_3}}$$

where J is the flux of sugar and T is a constant proportional to the number of carriers in the membrane. If K_1 is greater than K_3 and $V_1T = V_2T$ then it can be seen that, as [ATP] is increased, the apparent K_m for uptake or exit of sugar approaches K_3 but that the V_{max} for transport (which is proportional to V_1T and V_2T) is unchanged. Although this model is an oversimplification in that the reaction of ATP with the transport system is likely to be more complicated, it can be equally well applied to the asymmetric mobile-carrier and two-component-carrier models for transport.

Comparison with other nerves

Most research concerned with the transport of sugars by mammalian nerves has concentrated on aspects of sugar transport in brain (Lund-Andersen, 1979). Here, the experimental difficulties associated with the measurement of uptake in brain slices

combined with the heterogeneity of the preparation make it difficult to carry out any systematic study of sugar transport. Perhaps the two most fruitful approaches have been to measure sugar fluxes in cultured cells (Edström, Kanje & Walum, 1975) or synaptosomes prepared from cerebral cortex (Diamond & Fishman, 1973). Even here the results are controversial since it is not clear whether sugar uptake is rate limiting for sugar metabolism (Bachelard, 1975) or whether the rate of sugar uptake is so rapid that sugar metabolism becomes rate limiting for sugar uptake (Lund-Andersen & Kjeldsen, 1977). If uptake is rate limiting measurements of glucose uptake ought to be reliable but if metabolism is limiting uptake will be underestimated.

In spite of these difficulties it has been possible to show that sugar uptake in cultured cells and rat cerebral cortex synaptosomes is passive and phloretin-sensitive. Furthermore, 2-deoxy-D-glucose uptake in synaptosomes is reduced by the metabolic poisons cyanide and dinitrophenol (Diamond & Fishman, 1973). These results compare well with the findings in squid axons.

The intraneuronal glucose content of mammalian brain is not known. Some estimates suggest that the intracellular glucose concentration is close to that of the perineuronal space (Lund-Andersen, 1979) whereas others indicate that the neuronal glucose content may be much lower than this (Bachelard, 1975). Under appropriate experimental conditions, substantial intracellular levels of glucose and 2-deoxy-D-glucose can be detected in brain (Lund-Andersen, 1979) and in this respect, the squid axon and brain tissue may be similar. Within the brain, this might permit less active neurones to provide sugar for the more active nerve cells under conditions of glucose shortage.

We wish to express our thanks to the Director and the staff of the Laboratory of the Marine Biological Association, Plymouth for much help in the provision of material and facilities. We also wish to thank Dr R. J. Naftalin and Dr T. J. B. Simons for helpful discussion and the Medical Research Council for financial support.

REFERENCES

BACHELARD, H. S. (1975). How does glucose enter brain cells? In *Alfred Benzon Symp. VIII, Brain Work*, ed. INGVAR, D. H. & LASSEN, N. A., pp. 126–141. Copenhagen: Munksgaard.

BAKER, G. F. & WIDDAS, W. F. (1973). The asymmetry of the facilitated transfer system for hexose in human red cells and the simple kinetics of a two component model. *J. Physiol.* **231**, 143–165.

BAKER, P. F. & CARRUTHERS, A. (1981). Sugar transport in giant axons of *Loligo*. *J. Physiol.* **316**, 481–502.

BAKER, P. F., HODGKIN, A. L. & RIDGWAY, E. B. (1971). Depolarization and calcium entry in squid giant axons. *J. Physiol.* **218**, 709–755.

BAKER, P. F., HODGKIN, A. L. & SHAW, T. I. (1962). Replacement of the axoplasm of giant nerve fibres with artificial solutions. *J. Physiol.* **164**, 330–354.

BAKER, P. F. & POTASHNER, S. J. (1973). The role of metabolic energy in the transport of glutamate by invertebrate nerve. *Biochim. biophys. Acta* **318**, 123–139.

BOWYER, F. & WIDDAS, W. F. (1958). The action of inhibitors on the facilitated hexose transfer system in erythrocytes. *J. Physiol.* **141**, 219–232.

BRINLEY, F. J. JR. & MULLINS, L. J. (1967). Sodium extrusion by internally dialysed squid axons. *J. gen. Physiol.* **50**, 2303–2331.

BRINLEY, F. J. JR., SPANGLER, S. G. & MULLINS, L. J. (1975). Calcium and EDTA fluxes in dialysed squid axons. *J. gen. Physiol.* **66**, 223–250.

BRITTON, H. G. (1957). The permeability of the human red cell to labelled glucose. *J. Physiol.* **135**, 61–62*P*.

BRITTON, H. G. (1964). The permeability of the human red cell to labelled glucose. *J. Physiol.* **170**, 1–20.

DIAMOND, I. & FISHMAN, R. A. (1973). High affinity transport and phosphorylation of 2-deoxy-D-glucose in synaptosomes. *J. Neurochem.* **20**, 1533–1542.

DI POLO, R. (1977). Characterisation of the ATP-dependent Ca efflux in dialysed squid giant axons. *J. gen. Physiol.* **69**, 795–813.

EDSTRÖM, A., KANJE, M. & WALUM, E. (1975). Uptake of 3-*O*-methylglucose into cultured human glioma cells. *J. Neurochem.* **24**, 395–401.

GECK, P. (1971). Properties of a carrier model for the transport of sugars by human erythrocytes. *Biochim. biophys. Acta* **242**, 462–472.

HODGKIN, A. L. & KEYNES, R. D. (1955). The potassium permeability of a giant nerve fibre. *J. Physiol.* **128**, 61–88.

LACKO, L., WITTKE, B. & KROMPHARDT, H. (1972). Zur Kinetik der Glucose-Aufnahme in Erythrocyten. *Eur. J. Biochem.* **25**, 447–454.

LEFEVRE, P. G. (1948). Evidence of active transfer of certain non-electrolytes across the human red cell membrane. *J. gen. Physiol.* **31**, 505–527.

LEVINE, M., OXENDER, D. L. & STEIN, W. D. (1965). The substrate-facilitated transfer of the glucose carrier across the human erythrocyte membrane. *Biochim. biophys. Acta* **109**, 151–163.

LIEB, W. R. & STEIN, W. D. (1970). Quantitative predictions of a non-carrier model for glucose transport across the human red cell membrane. *Biophys. J.* **10**, 585–605.

LIEB, W. R. & STEIN, W. D. (1974). Testing and characterising the simple carrier. *Biochim. biophys. Acta* **373**, 178–196.

LUND-ANDERSEN, H. (1979). Transport of glucose from blood to brain. *Physiol. Rev.* **59**, 305–352.

LUND-ANDERSEN, H. & KJELDSEN, C. S. (1977). Uptake of glucose analogues by rat brain cortex slices: membrane transport *vs.* metabolism of 2-deoxy-D-glucose. *J. Neurochem.* **29**, 205–211.

MAWE, R. C. & HEMPLING, H. G. (1965). The exchange of [^{14}C]glucose across the membrane of the human erythrocyte. *J. cell. comp. Physiol.* **66**, 95–104.

MILLER, D. M. (1968). The kinetics of selective biological transport. IV. Assessment of three carrier systems using the erythrocyte–monosaccharide transport data. *Biophys. J.* **8**, 1339–1352.

NAFTALIN, R. J. & HOLMAN, G. D. (1977). Sugar transport in human red cells. In *Membrane Transport in Red Cells* ed. ELLORY, J. C. & LEW, V. L. London: Academic Press.

REGEN, D. M. & MORGAN, H. E. (1964). Studies of the glucose-transport system in the rabbit erythrocyte. *Biochim. biophys. Acta* **79**, 151–166.

ROSENBERG, T. & WILBRANDT, W. (1957). Uphill transport induced by counterflow. *J. gen. Physiol.* **41**, 289–296.

SEN, A. K. & WIDDAS, W. F. (1962). Determination of the temperature and pH dependence of glucose transfer across the human erythrocyte membrane measured by glucose exit. *J. Physiol.* **160**, 392–403.

STOREY, K. B. & STOREY, J. M. (1978). Energy metabolism in the mantle muscle of the squid *Loligo pealii*. *J. comp. Physiol.* **123**, 169–175.

WIDDAS, W. F. (1952). Inability of diffusion to account for placental glucose transfer in the sheep and consideration of the kinetics of a possible carrier transfer. *J. Physiol.* **118**, 23–39.

WIDDAS, W. F. (1980). The asymmetry of the hexose transfer system in the human red cell membrane. *Curr. Top. Membranes & Transp.* **14**, 165–223.

WILBRANDT, W. (1954). Secretion and transport of non-electrolytes. *Symp. Soc. exp. Biol.* **8**, 136–162.